An almost subharmonic instability in the flow past rectangular cylinders

A. Chiarini, M. Quadrio & F. Auteri

September 2022, 14th European Fluid Mechanics Conference

Politecnico di Milano

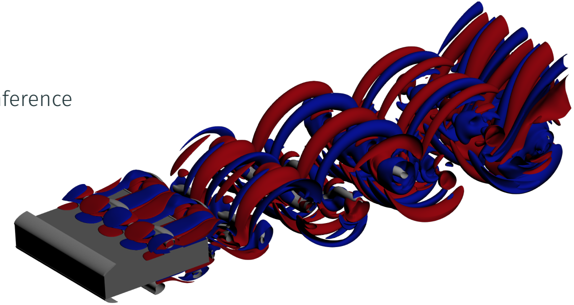

Flow past bluff bodies with sharp corners: the rectangular cylinder

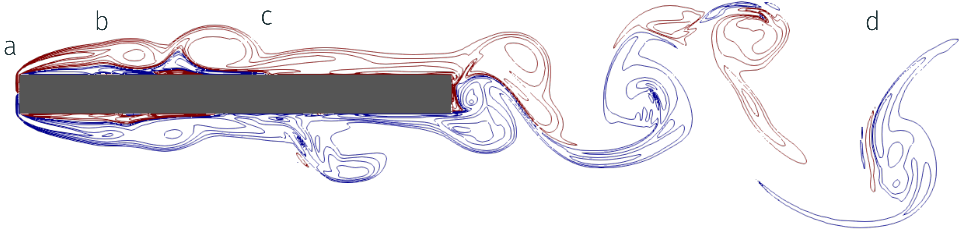

(a) Laminar separation at the corners

(b) Shear layers that may become unstable and reattach on the cylinder sides

(c) Several recirculating regions where flow instabilities may occur

(d) von Kàrmàn wake

The key flow parameters are: $\mathcal{AR} = L/D$ and $Re = U_\infty D/\nu$

The three-dimensional instability

The wake past short rectangular cylinders has been largely investigated

The three-dimensional instability

The wake past short rectangular cylinders has been largely investigated

- A and B synchronous wake Floquet modes are found for $\mathcal{A}\!\!R = 1$ (Blackburn & Lopez, PoF 2003)
- QP quasi-periodic mode is found at larger *Re* (Blackburn et al., JFM 2005)
- Other synchronous and quasi-periodic wake modes (A2 and QP2) arise for $\mathcal{A}\!\!R \leq 1$ (Choi & Yang, PoF 2014)

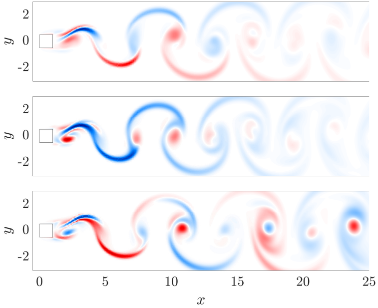

The three-dimensional instability

The wake past short rectangular cylinders has been largely investigated

- A and B synchronous wake Floquet modes are found for $\mathcal{AR} = 1$ (Blackburn & Lopez, PoF 2003)
- QP quasi-periodic mode is found at larger *Re* (Blackburn et al., JFM 2005)
- Other synchronous and quasi-periodic wake modes (A2 and QP2) arise for $\mathcal{AR} \leq 1$ (Choi & Yang, PoF 2014)

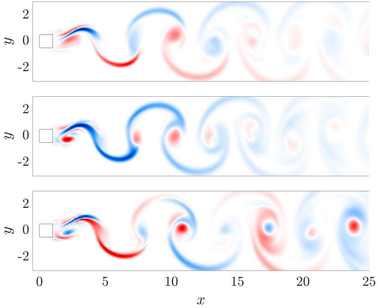

How does the three-dimensional instability change for elongated cylinders, when the flow reattaches over the longitudinal side?

Two-dimensional vortex shedding

For elongated cylinders the number n of LE vortices over the cylinder side increases with $A\!\!\!R$, defining different shedding modes

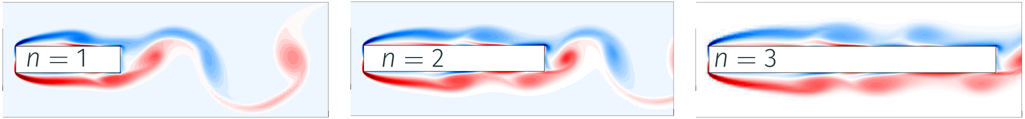

This leads to jumps in $St_L - A\!\!\!R$

$$St_L = fL/U_\infty$$

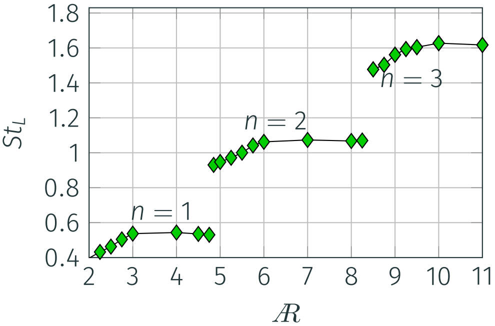

Two-dimensional vortex shedding

For elongated cylinders the number n of LE vortices over the cylinder side increases with $A\!\!\!R$, defining different shedding modes

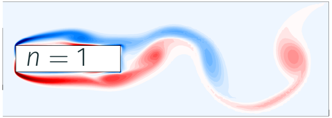

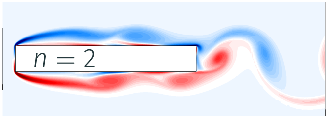

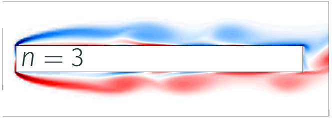

This leads to jumps in $St_L - A\!\!\!R$

$$St_L = fL/U_\infty$$

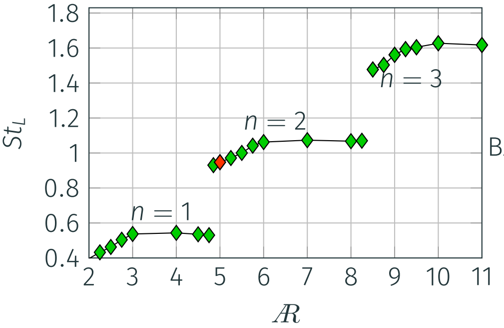

$A\!\!\!R = 5$
BARC benchmark

Floquet multipliers

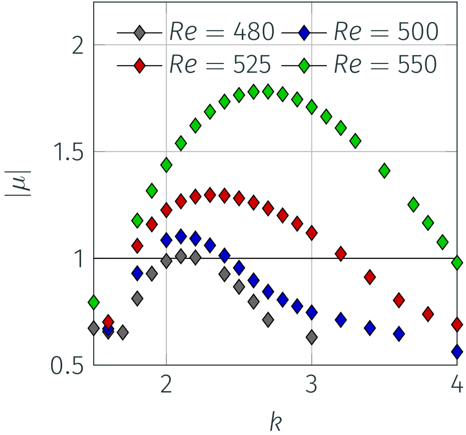

Floquet multipliers

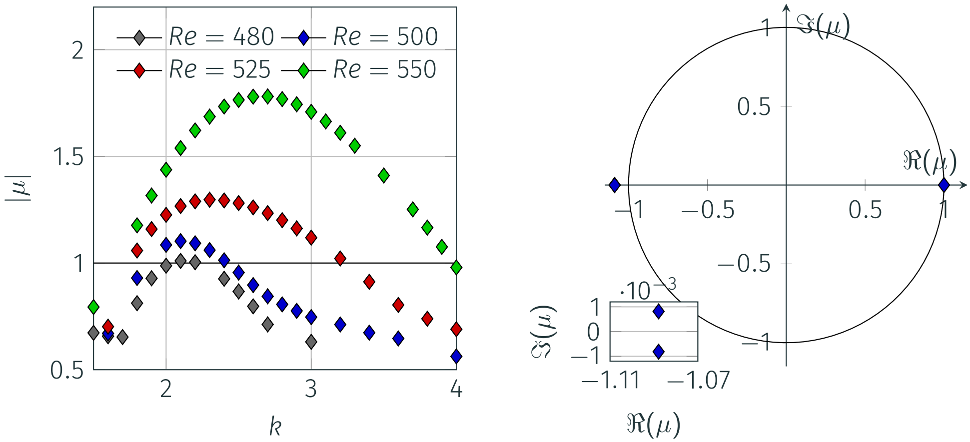

A quasi subharmonic (QS) unstable mode

Unstable mode

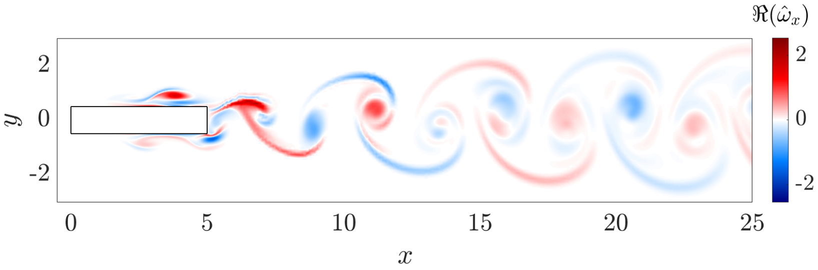

- Sign of the vorticity changes from one period to the next one
- $\Re(\hat{\omega}_x) \neq 0$ over the cylinder side

Non-linear three-dimensional Direct Numerical Simulation

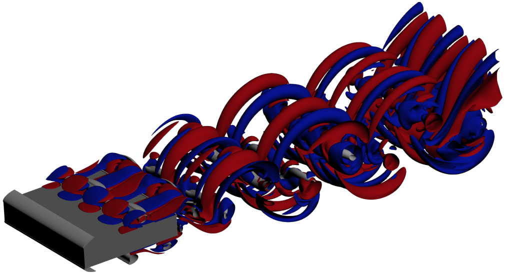

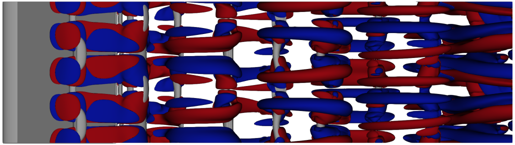

Non-linear three-dimensional Direct Numerical Simulation

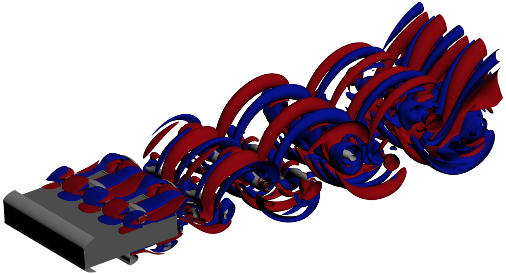

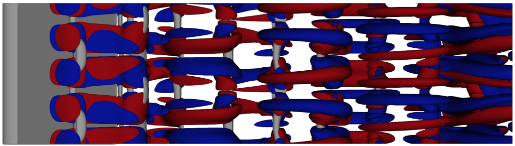

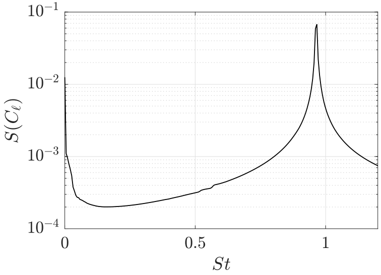

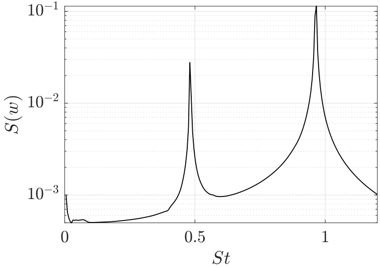

Three-dimensional flow

Pattern of staggered-arranged hairpin vortices like in a flat plate

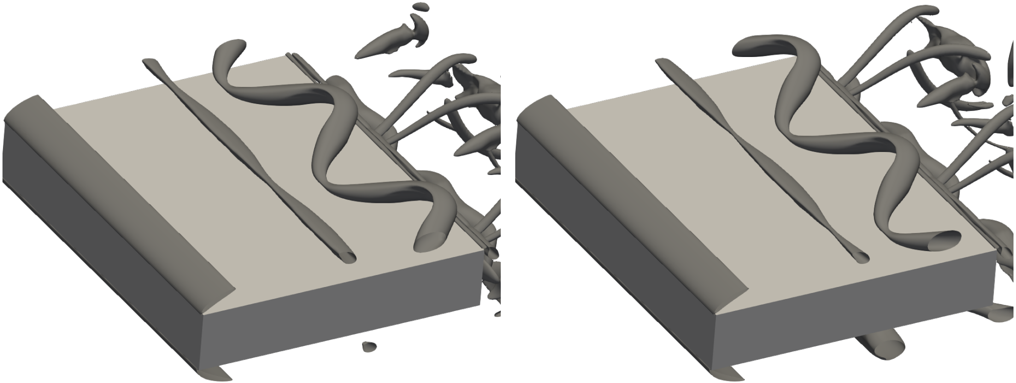

t $\qquad$ $t + T$

Structural sensitivity Giannetti, Camarri, & Luchini JFM 2010

$$I(x, y, k, t) = \frac{\hat{\boldsymbol{f}}^{+}(x, y, k, t)\hat{\boldsymbol{u}}(x, y, k, t)}{\int_t^{t+T} \int_\Omega \hat{\boldsymbol{f}}^{+} \cdot \hat{\boldsymbol{u}} \mathrm{d}\Omega \mathrm{d}t}$$

- Localises the wavemeaker region

Structural sensitivity Giannetti, Camarri, & Luchini JFM 2010

$$I(x, y, k, t) = \frac{\hat{f}^{+}(x, y, k, t)\hat{u}(x, y, k, t)}{\int_t^{t+T} \int_\Omega \hat{f}^{+} \cdot \hat{u} \mathrm{d}\Omega \mathrm{d}t}$$

- Localises the wavemeaker region over the longitudinal sides

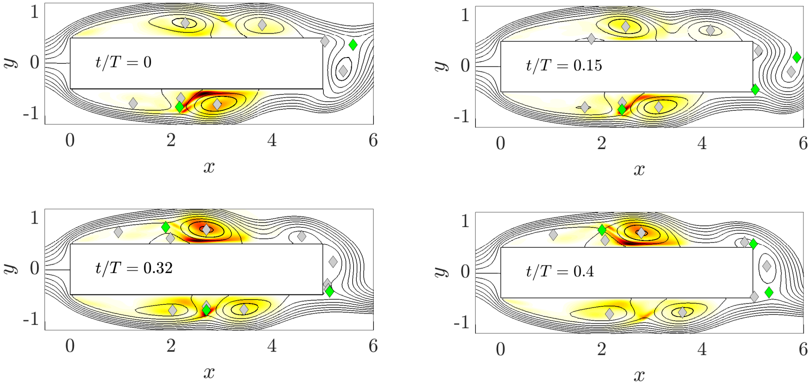

Structural sensitivity Giannetti, Camarri, & Luchini JFM 2010

$$I(x,y,k,t) = \frac{\hat{f}^{+}(x,y,k,t)\hat{u}(x,y,k,t)}{\int_t^{t+T}\int_\Omega \hat{f}^{+}\cdot\hat{u}\,\mathrm{d}\Omega\mathrm{d}t}$$

- Localises the wavemeaker region over the longitudinal sides

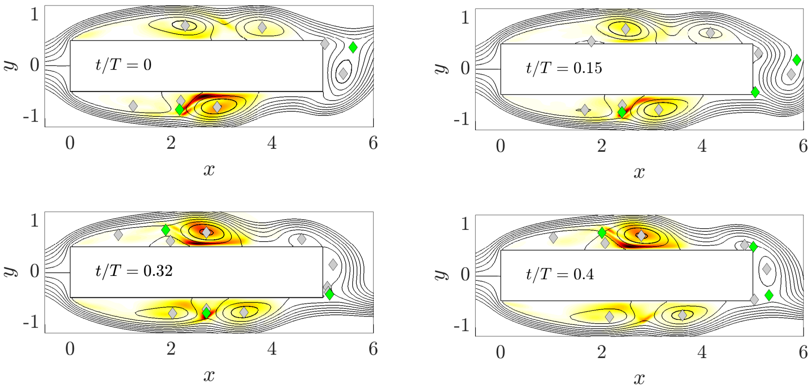

The QS mode is not an unstable mode of the wake

Is this an elliptic instability of the LE vortices?

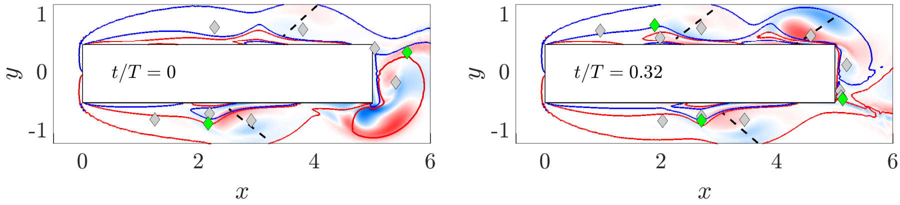

- Maximum perturbation in the base-flow vortex cores
- $\hat{\omega}_z$ has the typical two-lobe structures (Waleffe, 1990)
- Centres of the two lobes aligned at approximately 45° w.r.t. the ellipses axis

Is this an elliptic instability of the LE vortices?

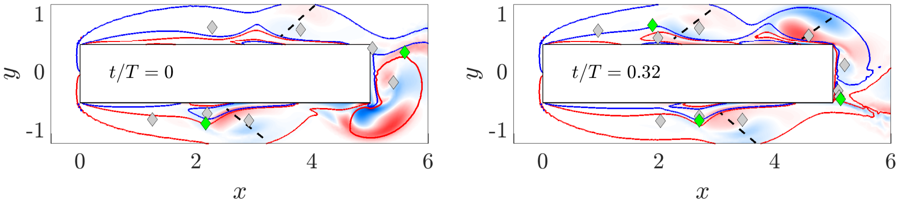

- Maximum perturbation in the base-flow vortex cores
- $\hat{\omega}_z$ has the typical two-lobe structures (Waleffe, 1990)
- Centres of the two lobes aligned at approximately 45° w.r.t. the ellipses axis

- The time scale of the base flow vortices are not consistent with a quasi-subhamronic instability
- This instability is not observed for $\mathcal{AR} \leq 4.8$ where $n = 1$

Physical mechanism

- Purely inviscid mechanism that results from the interaction between the vortices over the side
- First identified by Pierrehumbert & Widnall (JFM, 1982) for periodic shear layer vortices
- When a wall is present, the fastest growing disturbances are subharmonic in space and three-dimensional (Robinson & Saffman, JFM 1982)

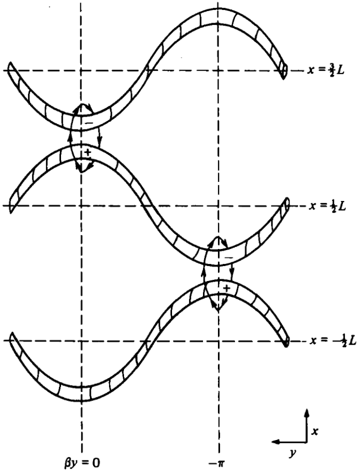

Pierrehumbert & Widnall (JFM, 1982)

Conclusions

- Three-dimensional instability of the flow past elongated rectangular cylinders
- A new quasi subharmonic (QS) unstable mode with $\lambda \approx 3D$ has been detected
- The triggering mechanism is inviscid and embedded in the interaction between LE vortices simultaneously placed over the cylinder side

Conclusions

- Three-dimensional instability of the flow past elongated rectangular cylinders
- A new quasi subharmonic (QS) unstable mode with $\lambda \approx 3D$ has been detected
- The triggering mechanism is inviscid and embedded in the interaction between LE vortices simultaneously placed over the cylinder side
- The secondary instabilities found for short cylinders can not be generalised

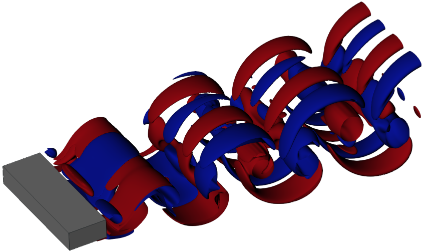

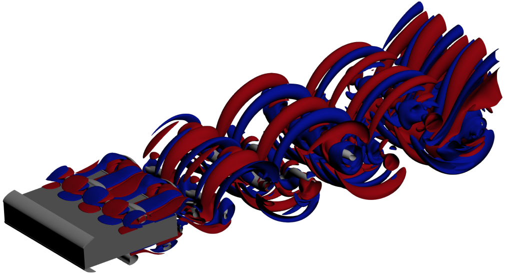

Conclusions

- Three-dimensional instability of the flow past elongated rectangular cylinders
- A new quasi subharmonic (QS) unstable mode with $\lambda \approx 3D$ has been detected
- The triggering mechanism is inviscid and embedded in the interaction between LE vortices simultaneously placed over the cylinder side
- The secondary instabilities found for short cylinders can not be generalised

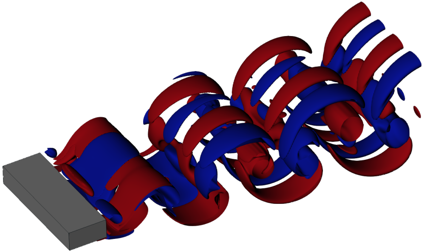

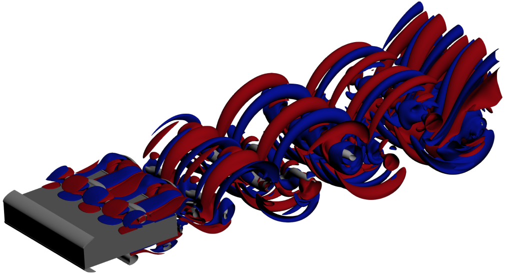

Thanks for listening!

Computational domain

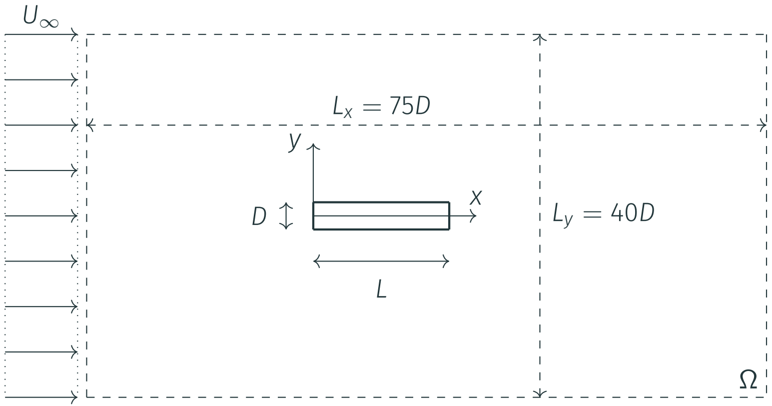

- $-25D \leq x \leq 75D$ and $-20D \leq y \leq 20D$
- 1.2×10^5 triangles, with 200 and 100 elements over the longitudinal and vertical sides of the cylinder

Methods I

Two-dimensional flow:

- FreeFem ++
- Third-order low-storage Runge–Kutta method for the nonlinear term, combined with an implicit second–order Crank-Nicolson scheme for the linear terms
- P2 elements for the vleocity and P1 elements for the pressure
- BoostConv (Citro et al, JCP 2017) algorithm has been employed to accelerate convergence

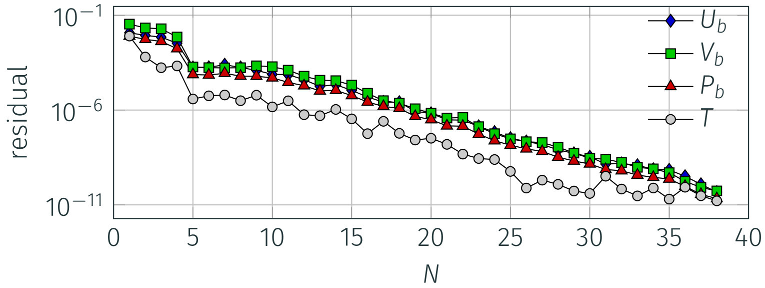

Methods II

Floquet analysis:

We can write:

$$\boldsymbol{u}_k(t_0 + T) = P_k \boldsymbol{u}_k(t_0)$$

And the eigenvalues of P_k are the Floquet multipliers μ

- Arnoldi method to compute the eigenvalues of P_k with largest modulus
- Modified Gram-Schmidt algorithm for the orthogonalisation of the eigenvectors
- For time integration same scheme as before

Methods III

Three-dimensional Direct Numerical Simulation:

- Second-order finite differences on a Staggered grid
- DNS code introduced by Luchini (2016)
- Fractional-step for the momentum equation with a third-order Runge–Kutta scheme
- The Poisson equation for the pressure is solved using an interative SOR algorithm
- The cylinder is considered with an immersed-boundary method
- $-30D \leq x \leq 80D$, $-25D \leq y \leq 25D$ and $0 \leq z \leq 2\pi D$
- $N_x = 1072$, $N_y = 590$ and $N_z = 200$, with 270 and 170 points over the longitudinal and vertical sides of the cylinder
- At the corners $\Delta x = \Delta y \approx 0.005D$

Unstable mode

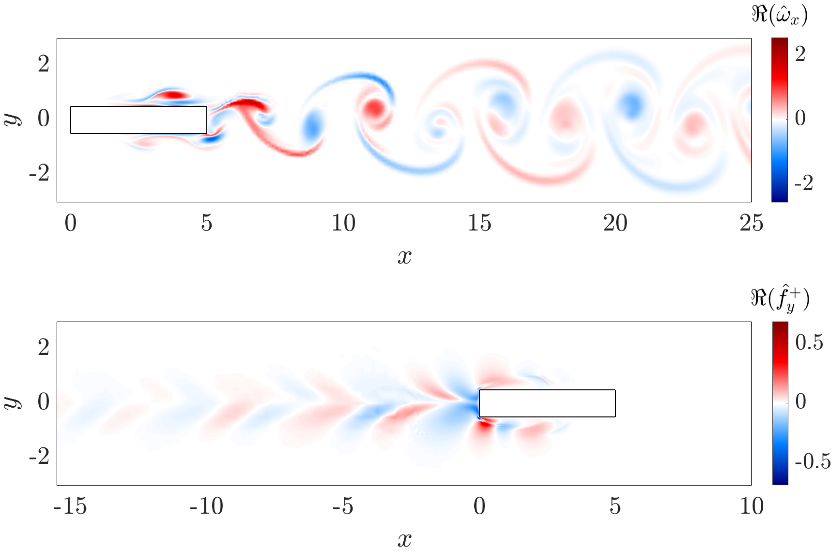

Other $\mathcal{AR}$

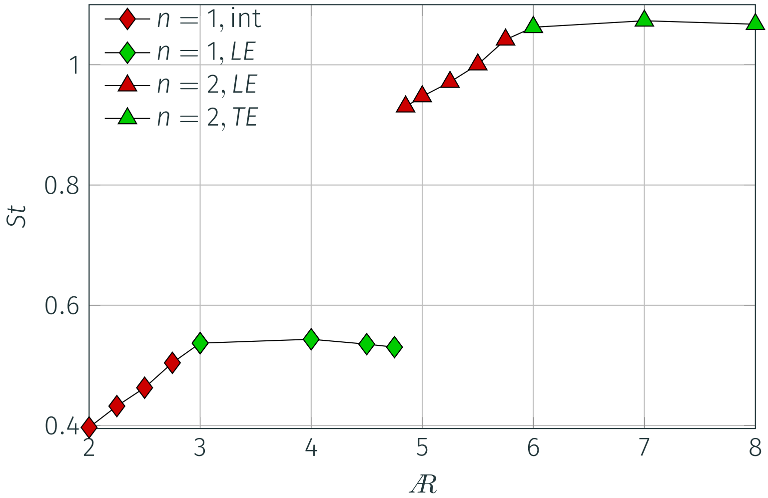

$3 \leq \mathcal{AR} < 4.85$

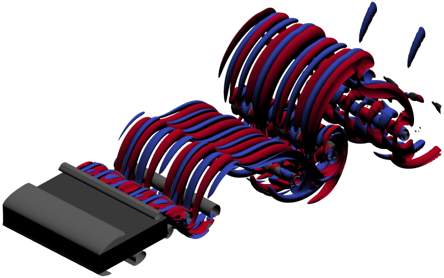

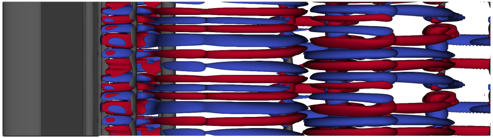

$4.85 \leq AR < 6$

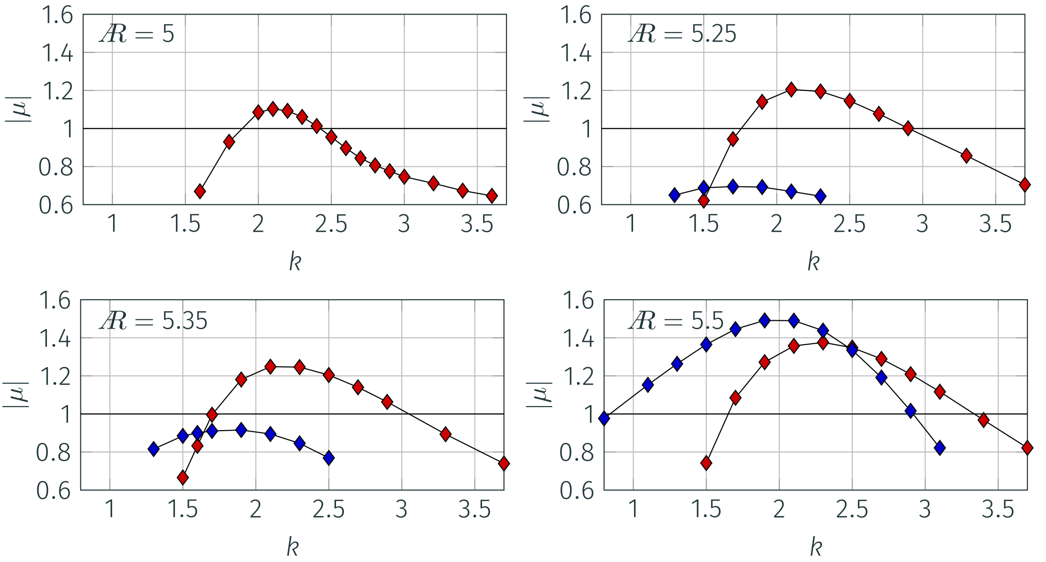

$\mathcal{AR} = 5.5$ at $Re = 450$

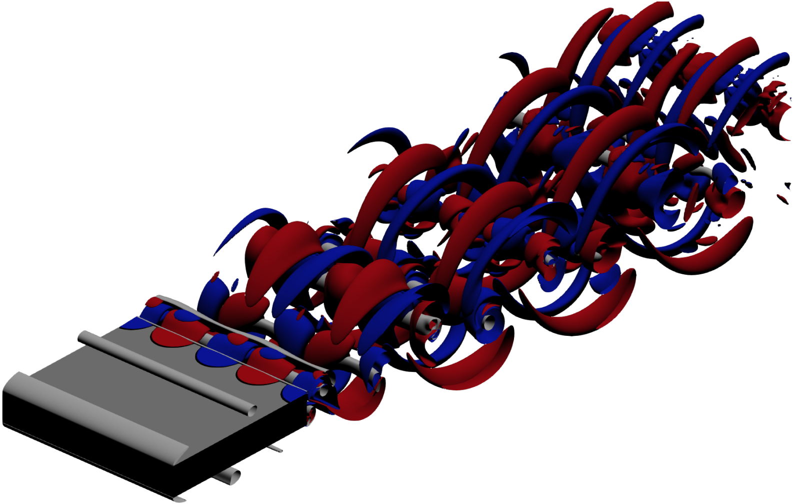

$\mathcal{AR} = 5.5$ at $Re = 500$

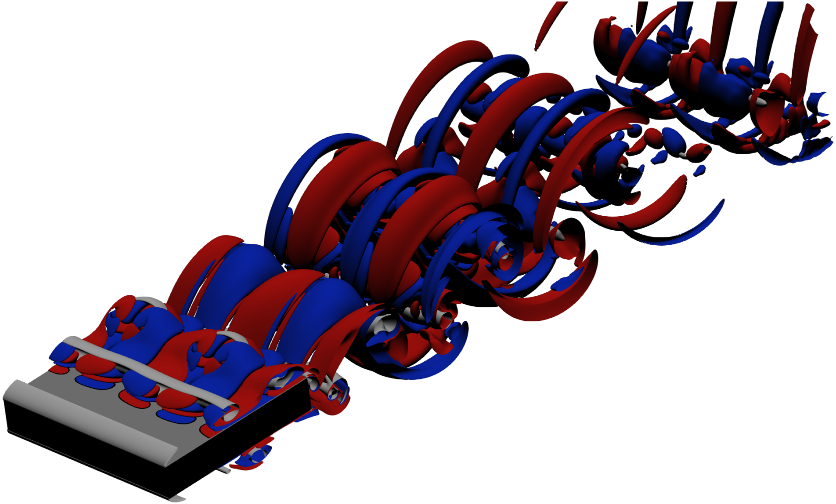

Two-dimensional vortex shedding

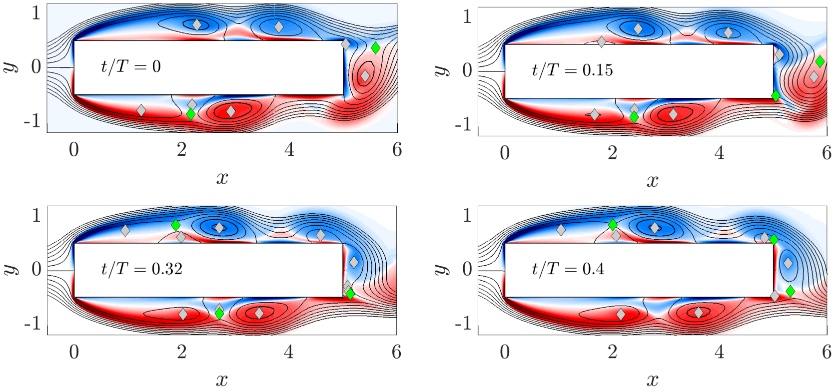

An hyperbolic stagnation point is required for vortex splitting (Boghosian & Cassel, 2016)

A quasi subharmonic mode

Systems with a spatio-temporal symmetry can not undergo a period-doubling codimension-one bifurcation (Swift & Wisenfeld, PRL 1984)

A quasi subharmonic mode

Systems with a spatio-temporal symmetry can not undergo a period-doubling codimension-one bifurcation (Swift & Wisenfeld, PRL 1984)

Introducing a small perturbation at the inlet:

$$\begin{cases} U(y) = U_\infty(1 + 2\delta y/D) \\ V(y) = 0 \end{cases}$$

A quasi subharmonic mode

Systems with a spatio-temporal symmetry can not undergo a period-doubling codimension-one bifurcation (Swift & Wisenfeld, PRL 1984)

Introducing a small perturbation at the inlet:

$$\begin{cases} U(y) = U_\infty(1 + 2\delta y/D) \\ V(y) = 0 \end{cases}$$

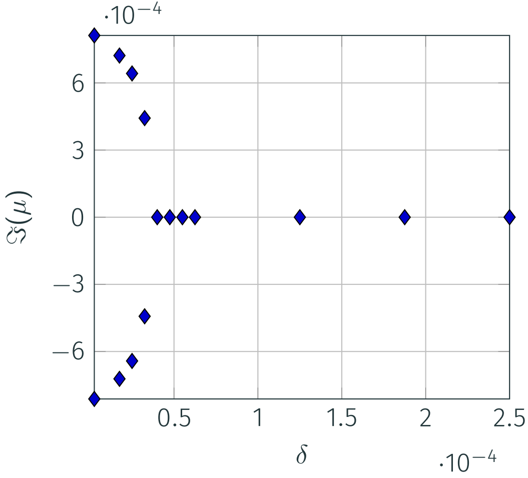

Floquet analysis for the three-dimensional instability

$$\{\boldsymbol{U}, P\}(x,y,z,t) = \underbrace{\{\boldsymbol{U}_b, P_b\}(x,y,t)}_{\text{Base flow}} + \underbrace{\frac{\epsilon}{\sqrt{2\pi}} \int_{-\infty}^{\infty} \{\boldsymbol{u}, p\}(x,y,k,t) e^{ikz} \mathrm{d}k}_{\text{Perturbation}}$$

The perturbation field has the functional form

$$\{\boldsymbol{u}, p\}(x,y,k,t) = \{\hat{\boldsymbol{u}}, \hat{p}\}(x,y,k,t) e^{\sigma t}$$

where

$$\{\hat{\boldsymbol{u}}, \hat{p}\}(x,y,k,t) = \{\hat{\boldsymbol{u}}, \hat{p}\}(x,y,k,t+T)$$

and

$$\{\boldsymbol{u}, p\}(x,y,k,t+T) = \{\boldsymbol{u}, p\}(x,y,k,t) e^{\sigma T}.$$

$\boxed{\mu = e^{\sigma T}}$ are the Floquet multipliers